A Null Hypothesis For CO_2

Roy Clark
Thousand Oaks

Summary

The energy transfer processes that occur at the Earth's surface are examined from first principles. The effect of small changes in the solar constant caused by variations in the sunspot cycles and small increases in downward long wave infrared flux due to a 100 ppm increase in atmospheric CO_2 concentration on surface temperature are considered in detail. The changes in the solar constant are sufficient to change ocean temperatures and alter the Earth's climate. The effects on surface temperature of small increases in downward LWIR flux are too small to be measured and cannot cause climate change. The assumptions underlying the use of radiative forcing in climate models are shown to be invalid. A null hypothesis for CO_2 is proposed that it is impossible to show that changes in CO_2 concentration have caused any climate change, at least since the current composition of the atmosphere was set by ocean photosynthesis about one billion years ago.

Introduction

Over the last 50 years, the atmospheric CO_2 concentration has increased by 70 ppm to ~380 ppm and the average annual sunspot index has been ~70% above its historical mean from 1650.[1-3] During this time, ocean temperatures have increased, Arctic sea ice extent has decreased and the average meteorological surface air temperature has increased.[4-8] Under ideal clear sky conditions, the 70 ppm increase in CO_2 increases the downward atmospheric long wave infrared (LWIR) surface flux by ~1.2 $W.m^{-2}$. This goes up to ~1.7 $W.m^{-2}$ for the full 100 ppm anthropogenic increase over the last 200 years. These numbers are derived from radiative transfer calculations using the HITRAN database and are used as 'radiative forcing constants' in the IPCC climate models.[9,10] SOHO/VIRGO satellite radiometer data show that the solar constant increased by ~1 $W.m^{-2}$ during the last solar sunspot cycle from a baseline of ~1365 $W.m^{-2}$.[11] The corresponding annual sunspot index changed from 8.6 to 120 and has now decreased again to 2.8.[3] This may be used to relate the change in the annual sunspot index to changes in the solar constant. An increase of 100 in the sunspot index produces an increase in the solar constant of ~1 $W.m^{-2}$. This means that the solar constant over the last 50 years (6 sunspot cycles) has been ~0.3 $W.m^{-2}$ above its historical average from 1650 The basic physics question is a simple one. How do these small changes in solar and LWIR flux influence the energy transfer process that occur at the Earth's surface and produce the observed climate changes? Since the air-ocean and air-land interfaces behave differently, it is convenient to consider them separately, starting with the air-ocean interface and some climate history.

The Air-Ocean Interface

During the last Ice Age, the solar constant was reduced by ~1 $W.m^{-2}$ because of changes in the ellipticity of the Earth's orbit due to Milankovitch cycles.[12] At the glacial maximum, sea level

was ~120 m lower than it is today.[13] This water was stored as ice at high latitudes. Over a 10,000 year period, the heat needed to melt this ice and warm the resulting water to 15 C requires an increase in the solar constant of ~0.4 $W.m^{-2}$. As the oceans warmed, the solubility of CO_2 decreased and the atmospheric CO_2 concentration increased from 200 to 280 ppm.[14, 15] This was an effect, not a cause of ocean warming. The Maunder Minimum was the period between 1645 and 1715 when there were almost no sunspots observed on the sun. This coincided with the 'Little Ice Age', a period of very cold winters. As the number of sunspots has increased since 1715, the Earth's climate has warmed up, as indicated by glacier melting and increases in sea level.[16] However, the atmospheric CO_2 concentration did not even begin to increase until after 1800.

The sun is the heat source for the Earth. Half of the solar energy is incident within the ± 30° latitude band and 70% is incident within ± 47°. The heating of the atmosphere in the tropics sets up the Hadley cell circulation and the trade winds. The trade winds in turn drive the large scale ocean gyres and the ocean currents such as the Gulf Stream that transport warm ocean water to higher latitudes. Under 'pristine' conditions, the sun can penetrate and warm the oceans to depths of 100 m. The ocean cools through a combination of evaporation and LWIR emission processes that are limited at most to a 1 mm surface layer. This evaporation is the primary heat source for the atmosphere above the ocean. The First Law of Thermodynamics only requires conservation of energy at the air-ocean interface. There is no local conservation of flux on any time scale. The solar heating of the ocean follows Beer's law. Sunlight is attenuated exponentially along the path length, depending on the local absorption/scattering coefficient. As the sun warms the ocean during the spring and summer, the upper layers heat up and a stable thermal gradient develops. As the ocean starts to cool in the fall, the upper layers cool first and a uniformly mixed layer develops that extends to lower depths as the temperature decreases. Two distinct solar heated layers form. Close to the surface, the ocean is mixed by diurnal thermal density gradients and wave action. The depth and time scales here are nominally 10 to 25 m and 24 hours. At lower depths, mixing occurs more slowly through thermal/salinity density gradient changes, since surface motions are only weakly coupled to these depths. The mixing scales are 25 to 100 m and a 'seasonal' 90 days or longer.

Historically, data on subsurface ocean temperatures, mixing and transport has been sparse. This situation has changed recently with the implementation of the Argo float program. This now provides high quality subsurface ocean temperature, salinity and density data using a fleet of 3000 submersible floats that are distributed throughout the world's oceans.[17] The floats are designed to sink to a depth of 1000 or 2000 m, drift at that depth for ten days, then return to the surface, acquiring data during the ascent. At the surface, the data are transmitted via satellite to a series of ground monitoring stations. The floats then repeat the descent/ascent cycle. The floats are not tethered and drift with the ocean currents. The principal features of the solar heating of the ocean at various latitudes through the year may be understood by examining the results from selected Argo floats. Figure 1 summarizes a year of data from 5 selected Argo floats covering a range of latitudes from the equator to the Antarctic Circle in the southern central Pacific Ocean. The temperatures at 5 depths, 5, 25, 50, 75 and 100 m are shown as a time series for the year. The latitude drift of the floats is also shown. Because of variability in the float actuators, the

depths are averages for each float with a standard deviation of approximately 0.2 m. The average latitude, longitude, depths and temperatures for each float are summarized in Table 1. The average temperatures show the expected decrease in temperature at higher latitudes.

Table 1: Argo float summary data

Float 1							
Serial No.	34250						
Av. Latitude	-1.5	Av. Depth m	4.6	23.4	49.5	74.4	99.3
Av. Longitude	126.2	Av. Temp. C	24.5	24.1	21.9	18.0	15.1
Float 2							
Serial No.	59033						
Av. Latitude	-20.9	Av. Depth m	4.4	24.3	52.2	75.2	99.2
Av. Longitude	105.2	Av. Temp. C	23.0	22.9	22.8	22.4	22.0
Float 3							
Serial No.	35605						
Av. Latitude	-42.4	Av. Depth m	4.6	24.3	52.3	75.2	99.3
Av. Longitude	153.5	Av. Temp. C	12.9	12.9	12.2	11.1	10.6
Float 4							
Serial No.	26893						
Av. Latitude	-52.7	Av. Depth m	4.4	27.3	51.1	75.2	99.2
Av. Longitude	146.5	Av. Temp. C	7.4	7.4	7.3	7.1	6.9
Float 5							
Serial No.	35987						
Av. Latitude	-63.4	Av. Depth m	4.8	23.6	50.8	73.2	96.5
Av. Longitude	140.7	Av. Temp. C	-0.5	-0.5	-0.6	-0.9	-1.0

Figure 1a shows the results from a float drifting near the equator. The average temperature at 5 m is 24.5 C. There is no obvious seasonal peak in the data. The temperatures at the 5 and 25 m levels are similar, so these levels are usually mixed. Mixing down to the 50 m level occurs approximately half of the time. However, the 75 and 100 m levels have temperatures that are on average 4 and 7 C below the 50 m level. These lower levels are rarely coupled to the surface. Figure 1b shows the results from a float drifting near 21.5° S. There is a distinct seasonal peak in March with the 5 m temperature reaching 25.5 C. (Seasons are opposite in the southern hemisphere). The temperatures then merge together as the ocean cools. All of the levels down to 100 m are fully mixed for 6 months. Figure 1c shows the results from a float drifting near 42.4° S. The temperature profiles show a similar pattern to the float at 21.5° S, but the temperatures are lower because of the higher latitude. The maximum 5 m temperature is 16 C. Figure 1d shows the results from a float drifting near 53° S. The overall temperatures are reduced compared the 42.4° S float. The maximum 5 m temperature is now 10 C and the duration of the summer separation of the subsurface layers is reduced to approximately 3 months. This float also drifted about 6° S from March to December, so there is an overall cooling from this drift superimposed on the seasonal variation. Figure 1e shows the results from a float drifting near 63.4° S, close to the Antarctic Circle. The average temperatures at all depths are below 0 C. The summer mixing depth pattern is similar to the previous 3 floats, but the temperature range is reduced. At all depths, the temperatures reach a minimum of -1.8 C from September to November. This is the freezing point of sea ice.

Annual time series of 10 day data for 5 selected Argo floats at a range of latitudes in the mid S. Pacific Ocean from the equator to the Antarctic. The temperatures at 5 depths, nominally 5, 25, 50, 75 and 100 m are shown. The latitude drifts of the floats are also shown. The separation of warm surface layers formed by spring and summer solar heating can be clearly seen at latitudes above 20°. Near the equator, the subsurface layers are not usually mixed. Heat may accumulate over long periods in these layers.
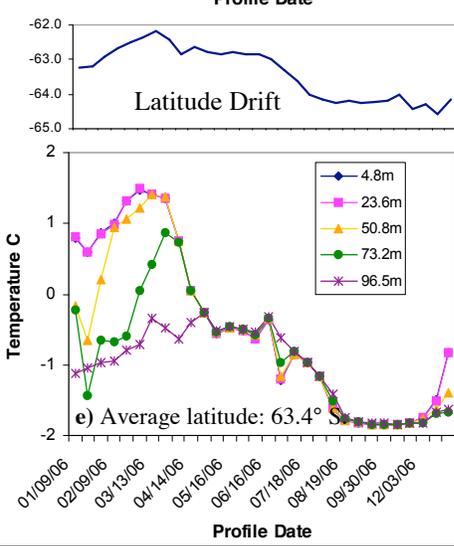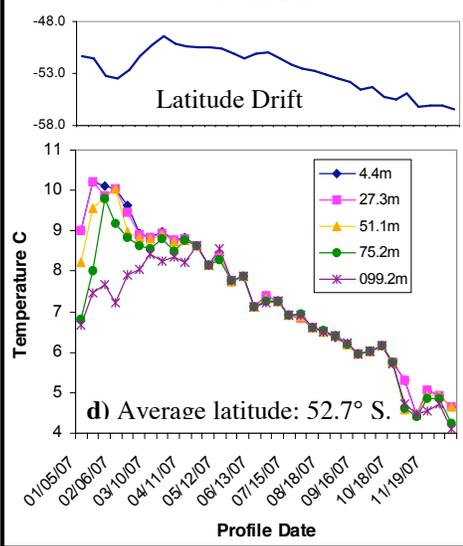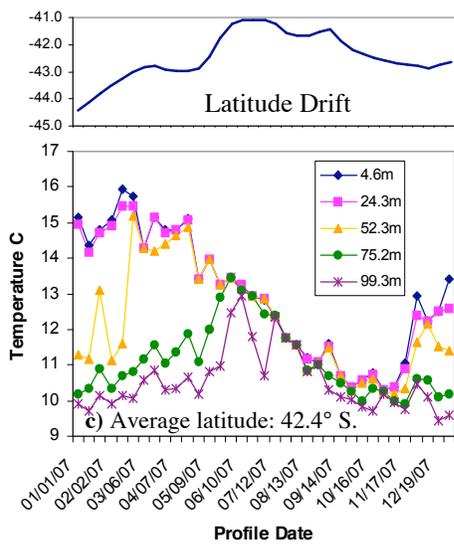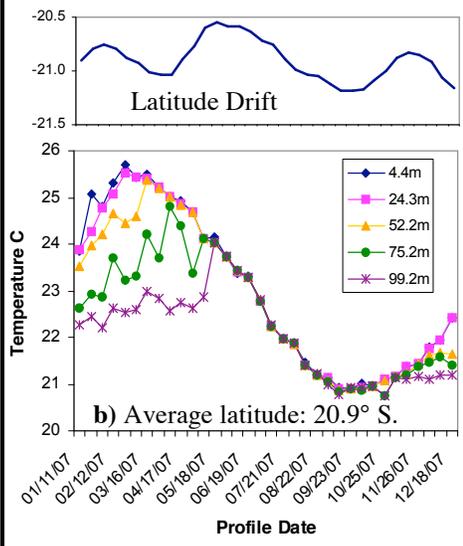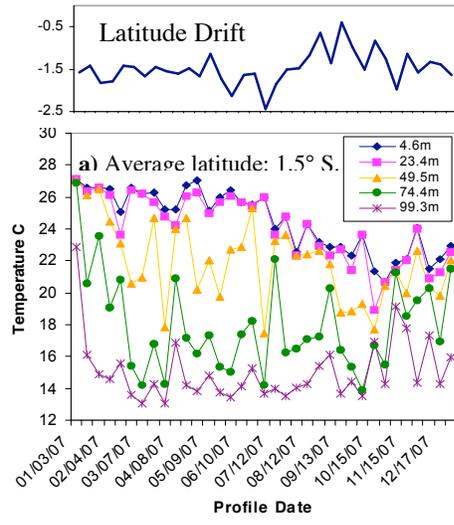
Figure 1: Selected Argo float data. (See text for further discussion).

The float data presented here illustrate the seasonal trends in subsurface ocean temperatures. During the summer, the lower subsurface layers are not coupled to the surface while they are warmed by solar illumination. Heat from these layers may be transported or re-circulated over long distances by wind driven ocean currents. At low latitudes, the diurnal and seasonal temperature variations may not be sufficient to mix these subsurface layers at all and heat may accumulate at these depths for extended periods. At higher latitudes, the ocean cools and the subsurface layers are coupled to the surface during the winter months. The ocean has to cool to - 1.8 C for ice to form. It is also important to note that at high latitudes, the surface area of a spherical zone decreases significantly. This geometric factor increases the depth of ocean currents as they flow to higher latitudes, further limiting their interaction with the surface. Small changes in subsurface ocean temperatures can therefore result in large changes in polar ice formation. No interaction with the atmosphere is required and changes in atmospheric CO_2 concentrations can have no effect on this process.

The solar heating of the ocean may be simulated using a simple Beer's law model as illustrated in Figure 2. This was used to determine ocean solar heating and cooling as a function of depth over a 1 year period at 30° latitude with the solar constant set to 1365 W.m^{-2}. The model depth resolution was 1 m and the time step was 0.5 hours. The calculated results are shown in Figure 3. They are consistent with Argo Float data such as the examples shown in Figure 1. The model was then extended to simulate changes in the solar constant due to the sunspot cycle from 1650 to 2000 using a scale factor of 1 W.m^{-2} per 100 change in the annual sunspot index.[11] The calculated change in ocean temperatures at 90 m depth is shown in Figure 4. There is a distinct decrease to the end of the Maunder Minimum followed by an overall increase of almost 0.5 C from 1750 to 2000. This simple model clearly demonstrates that small changes in the solar constant influence ocean temperatures and cause climate change. Subsurface ocean layers are transported over long distances by wind driven ocean currents without any interaction with the surface. The average global ocean temperature increase for the 0 to 300 m depth level from 1953 to 2003 was 0.17 C.[4] This is consistent with Figure 4 over the same time period. However, there was also significant variation in temperatures between ocean basins. The N. Atlantic warmed by 0.35 C, the N. Pacific by 0.09 C. These fluctuations are caused by differences in ocean circulation, mixing and wind speed.[5]

It is also straightforward to show that a 1.7 W.m^{-2} increase in downward LWIR flux at the ocean surface cannot change ocean temperatures. Water is almost completely opaque to LWIR radiation.[18] The LWIR absorption/emission depth is less than 1 mm, so the interaction volume is at most 10 cm^3. An increase in downward LWIR flux at the ocean surface of 1.7 W.m^{-2} heats the surface layer at a rate of at least 2.4 C per minute. The ocean responds by rapidly increasing the surface evaporation rate by 1.7 W.m^{-2}, or 2.7 g.hr^{-1} of water for ideal 'clear sky' conditions. This corresponds to a 2.4 cm.yr^{-1} increase in evaporation rate since 1800, with 1.7 cm.yr^{-1} of this increase occurring over the last 50 years. Global estimates of ocean evaporation rates show that between 1977 and 2003 the global ocean evaporation rate has increased from 103 to 114 cm.yr^{-1} with an uncertainty of ±2.72 cm.yr^{-1}.[19] This was caused by a 0.1 m.s^{-1} increase in average wind

speed. The 'clear sky' upper limit for the CO_2 induced increase in evaporation is below the measurement uncertainty bounds. Long term averages of surface air temperatures are ~2 C below the corresponding ocean surface temperatures.[20] This means that there is usually no direct heating of the ocean by the atmosphere, as required by the Second Law of Thermodynamics. The latent heat of evaporation is not released until the water condenses, which is generally at an altitude above 1 km. It is therefore impossible for an increase in downward atmospheric LWIR flux of 1.7 W.m^{-2} to heat the ocean. The increase in flux is converted by the ocean surface into an insignificant change in evaporation rate. This is buried in the noise of wind induced fluctuations in evaporation and changes in LWIR flux caused by variations in aerosols, clouds and near surface humidity.

The solar heating of the first 100 m of the ocean is calculated every 0.5 hr and the 1m layers are mixed according to temperature. The solar intensity algorithm was adapted from IEEE Standard 738 (1993). A constant LWIR cooling flux was used so that the model repeats each year. The solar attenuation for $\alpha = 0.075$ m^{-1} as used in the model is also shown.
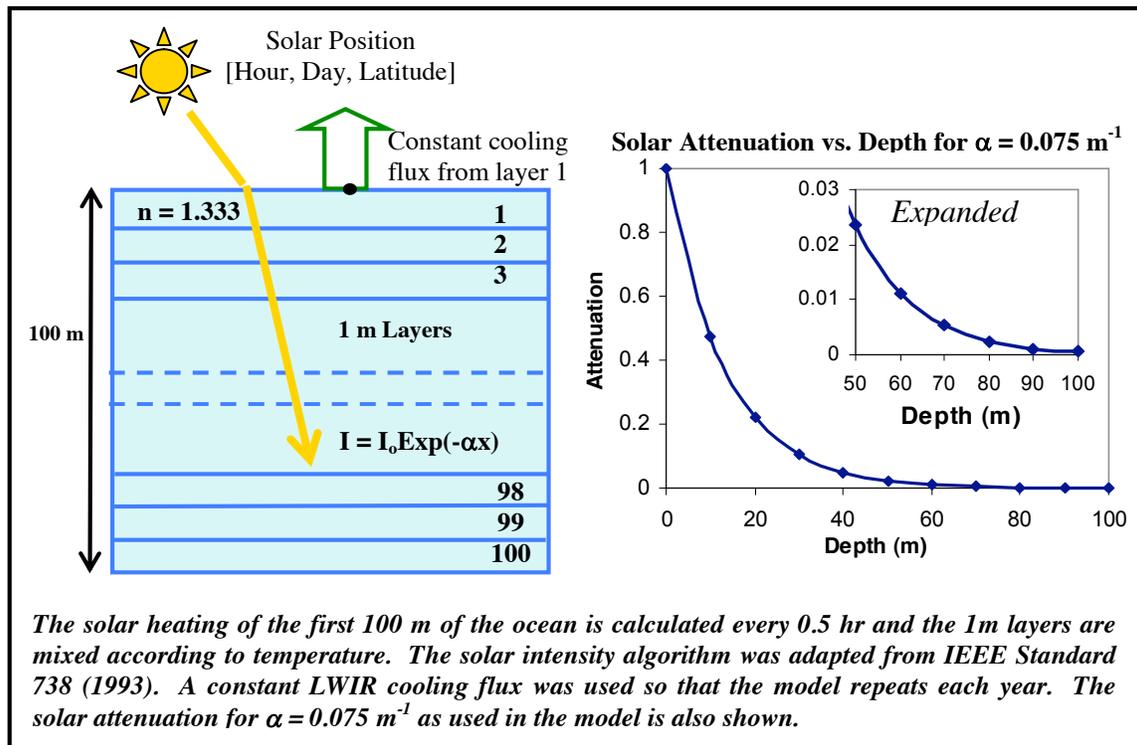
Figure 2: Simple ocean solar heating model base on Beer's Law

Ocean layer solar heating to 100 m depth calculated over a 1 year period for 30° latitude. As the ocean heats up in the spring and summer, stable layers form. As the ocean cools in the fall and winter, the heated layers cool from the surface down. Inset shows the diurnal mixing layer and the initial heated layer separation
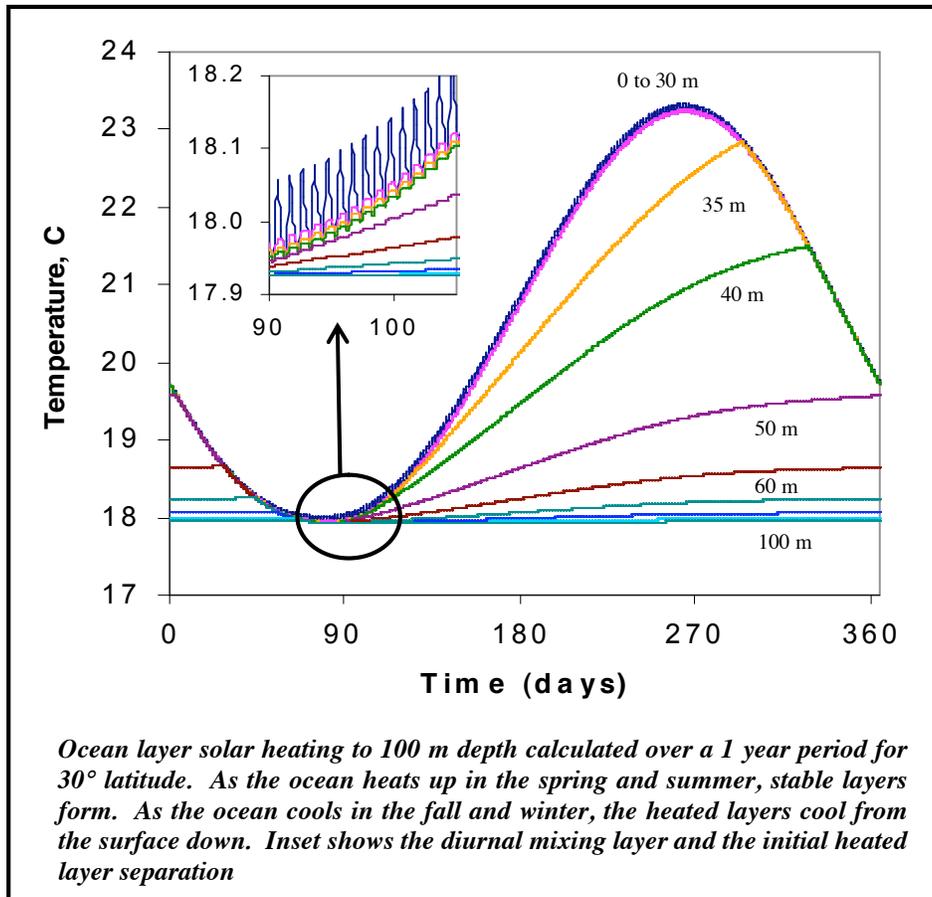
Figure 3: Ocean layer solar heating model results

Calculated change in ocean temperatures at 90 m depth using the sunspot index to set the solar constant. Mean solar constant was 1635 $W.m^{-2}$. A 1 $W.m^{-2}$ increase in solar constant for a 100 increase in index was used in the model. The cooling during the Maunder Minimum and the current warming period are clearly demonstrated.
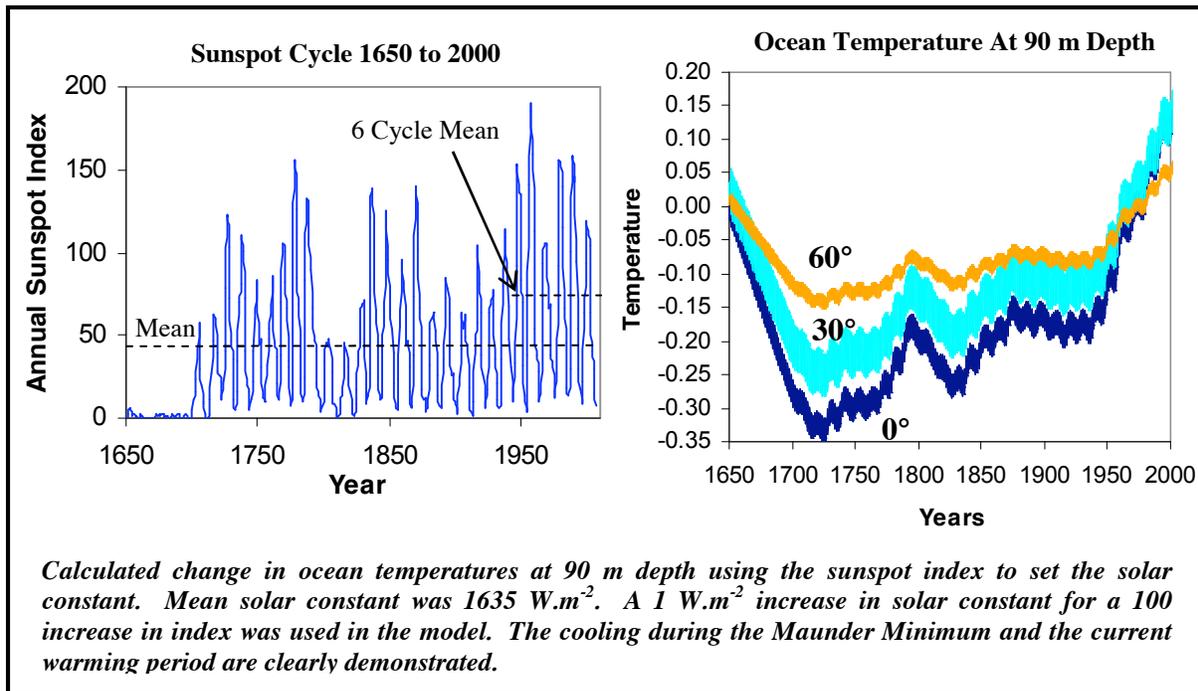
Figure 4: Calculated sunspot induced changes in ocean temperatures at 90 m depth, 1650 to 2000.

The Air-Land Interface

The ground is heated by the sun during the day and the increase in LWIR flux from the warm surface heats the air. It is important to distinguish clearly between the actual ground surface temperature and meteorological surface air temperature. The surface temperature needed for energy transfer analysis is the ground surface temperature. The meteorological surface air temperature is the air temperature measured in an enclosure placed 1.5 to 2 m above the ground.[21] There is no obvious or simple relationship between these two temperatures. Solar radiation is absorbed and reflected by the ground. The resulting surface temperature depends on the absorption coefficient, the thermal conductivity and heat capacity of the ground, the surface area and angles of incidence, the balance of the upward and downward LWIR flux and the direct air convection. If the ground is moist, latent heat effects also have to be included. The meteorological surface air temperature depends on the origin of the bulk air mass of the local weather system, surface LWIR flux heating, air convection and wind speed. As for the air-ocean interface, the First Law of Thermodynamics imposes energy conservation, but there is no requirement that the flux be conserved on any time scale. The Second Law of Thermodynamics requires that the heat transfer follow the thermal gradient.

Surface heating may be analyzed using a simple thermal conduction model analogous to the ocean heating model. This is illustrated in Figure 5. The results for summer and winter illumination of a concrete surface are shown in Figure 6. The calculated daily temperature excursions for summer and winter solar heating are 40 and 20 C at 35° latitude. A 1% increase in solar flux produces peak summer and winter temperature increases of 0.34 and 0.17 C. The increases in surface temperature due to a 1.7 $W.m^{-2}$ increase in LWIR flux vary between 0.14 and 0.36 C, with higher temperature increases observed at lower surface temperatures. These changes are for ideal 'clear sky' conditions over a period of 200 years. Variations in cloud cover, aerosols and humidity will produce fluctuations in LWIR flux that are much larger than 1.7 $W.m^{-2}$, so the effects of CO_2 on ground surface temperature are not measurable. However, no historical record of surface temperature is available, so the meteorological surface air temperature has been substituted for the surface temperature without any consideration of the differences between the two.
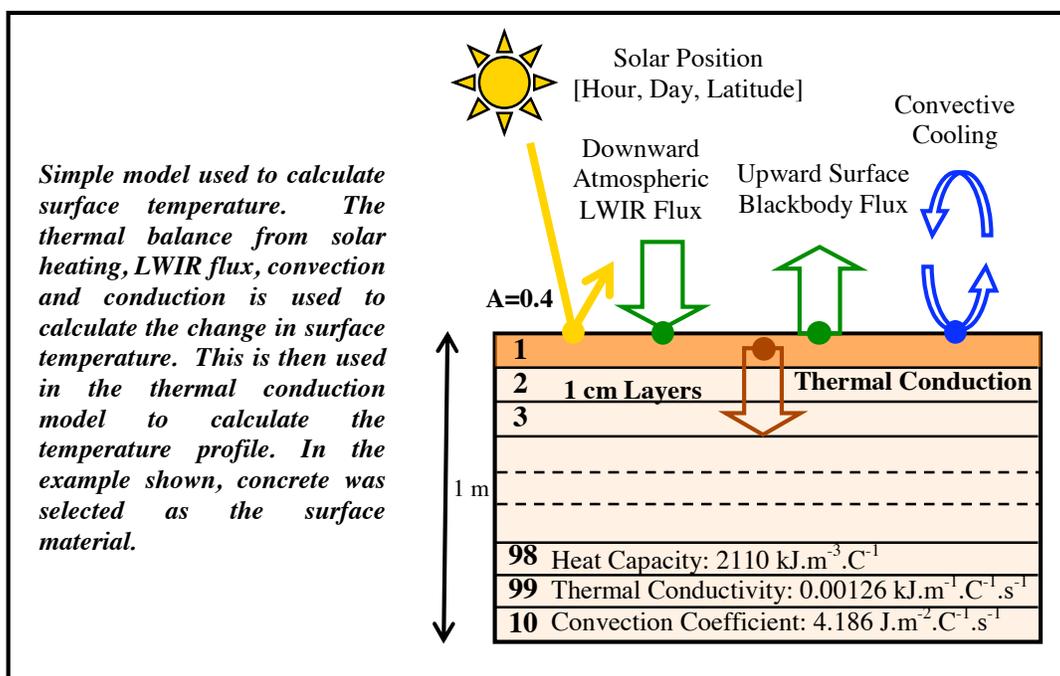
Figure 5: Simple land surface heating model

During the day the air is heated by the excess LWIR radiation from the ground. Figure 7 shows the spectrally resolved flux absorbed by H_2O and CO_2 as a function of height above the ground and Figure 8 shows the total flux absorbed vs. height derived from a high resolution (0.01 cm^{-1}) radiative transfer model.[9] The surface thermal gradient was set to 30 K with the surface temperature at 325 K and the air temperature at 295 K. In this case at 2 m above the ground, a total of flux of 16 W.m^{-2} is absorbed. Of this, only 1.6 W or 10 % is absorbed by CO_2. The radiative transfer model was also used to simulate the effect of changes in thermal gradient, CO_2 concentration and humidity on the heat transfer at 2 m above the ground. These are summarized in Figure 9. For a 30 K gradient, the change in flux produced when the CO_2 concentration is increased from 280 to 380 ppm is only 0.25 W.m^{-2}. As the humidity is changed from 10 to 90% for this case, the total absorbed flux changes from 8 to 20 W.m^{-2}. The meteorological surface air temperature records the effect of the surface LWIR heating (and cooling) of the air 2 m above the ground superimposed on the bulk air temperature of the local weather system. Based on the results presented in Figures 6 to 9, it is impossible to detect the effect of a 100 ppm increase in CO_2 concentration on the meteorological surface air temperature. This may also be illustrated by examining the so called US surface temperature anomaly as shown in Figure 10.[22] There is a distinct peak in the temperature anomaly in the 1930s due to the dust bowl drought. This is an indication of increased surface solar absorption and lower moisture levels. There is no relationship between the measured temperature anomaly and the calculated increase in surface temperature due to anthropogenic CO_2.

Daily summer and winter ground surface temperature variations, 35° latitude. Summer change is 40 C, winter is 20 C.

A 1% increase in solar flux increases peak summer temperature by 0.34 C and peak winter temperature by 0.17 C.

A 1.7 $W.m^{-2}$ increase in downward LWIR flux (+100 ppm CO_2) increases peak summer temperature by 0.32 C and winter temperature by 0.34 C. Maximum change occurs at night. Daytime increases are less, 0.14 and 017 C.

Figure 6: Land heating model results

Fraction of the LWIR flux absorbed by air layers near the ground. Surface temperature is 325 K, air temperature is 295 K, CO_2 concentration is 380 ppm, RH is 50%. Path lengths are from 0.5 m to 1 km. Flux fractions shown are derived from high resolution (0.01 cm^{-1}) radiative transfer calculations, H_2O and CO_2 only.
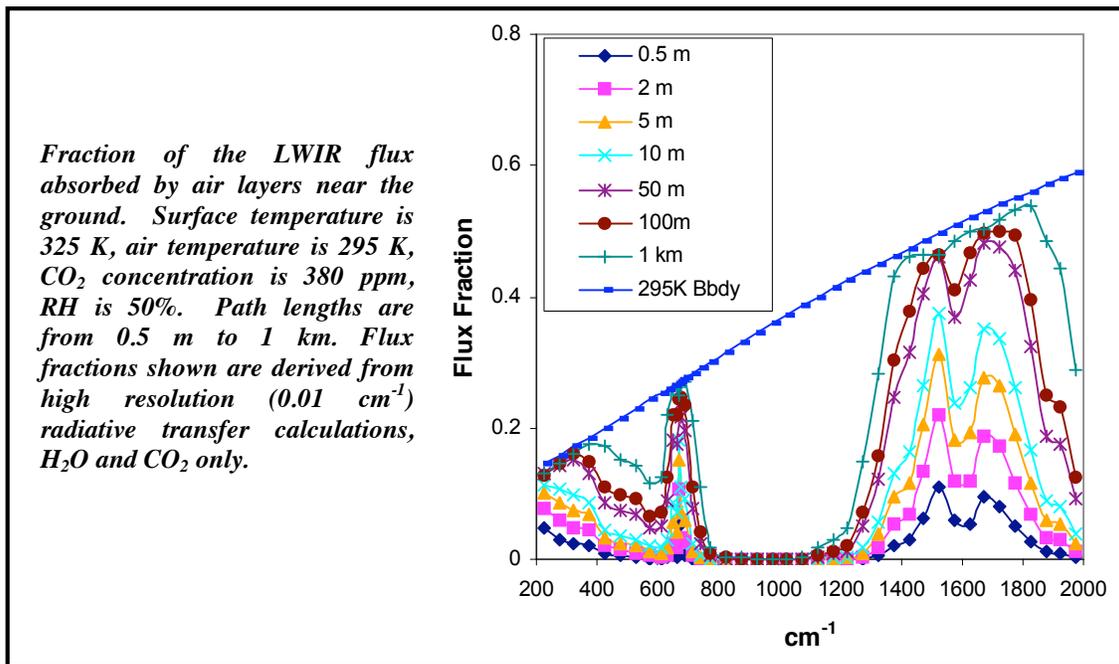
Figure 7: LWIR absorption near the air-land interface

(a) Total (cumulative) flux absorbed up to 1 km from the ground. The contributions to the absorption from H_2O and CO_2 are also shown separately. (b) The absorption from 0.5 to 10 m on an enlarged scale. Data derived from Figure 7. At 1 km, H_2O absorbs 75% of the flux. This increases at shorter path lengths to 90% at 2 m and 96% at 0.5 m.
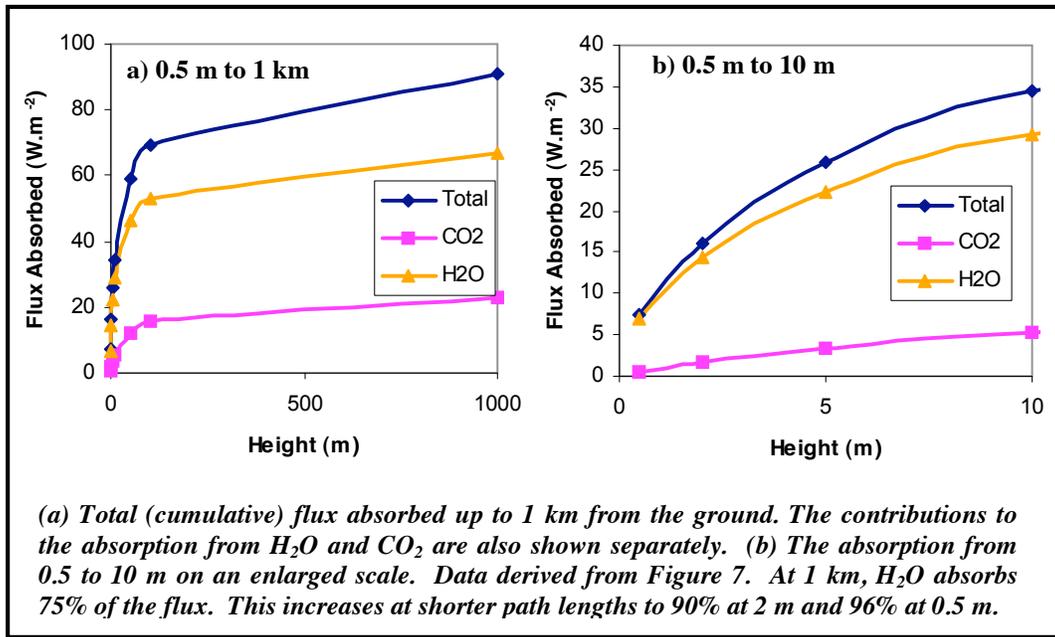
Figure 8: Cumulative total LWIR absorption

(a) There is a slight increase in the absorbed flux at 2 m above the ground when the CO_2 concentration is increased from 280 to 380 ppm. For a 30 K surface-air temperature difference it is still only 0.25 $W.m^{-2}$. (b) The corresponding change in flux for a change in RH from 10 to 90 % is 12 $W.m^{-2}$. For a thermal gradient of 2 K the RH flux change is reduced to 0.8 $W.m^{-2}$. For comparison, the flux changes due to a 100 ppm increase in CO_2 at 50% RH are 0.25 and 0.02 $W.m^{-2}$.

Figure 9: Effect of a 100 ppm increase in CO_2 concentration and changes in RH on the LWIR flux absorbed at 2m above the ground

11

U. S. temperature anomaly from 1880, 1 year and 5 year averages. The calculated increase in surface temperature for a 292K blackbody surface due to the increase in CO_2 is also shown. This is a cloud and aerosol free upper limit. There is clearly no relationship between the measured temperature anomaly and the calculated change in surface temperature.
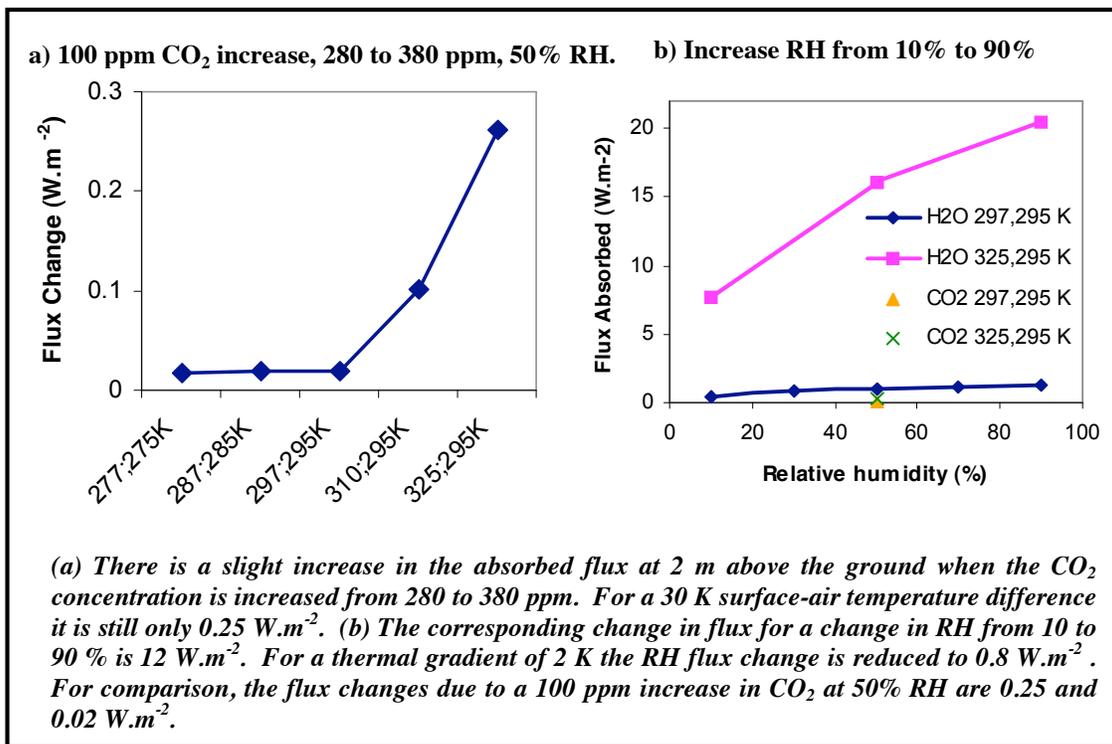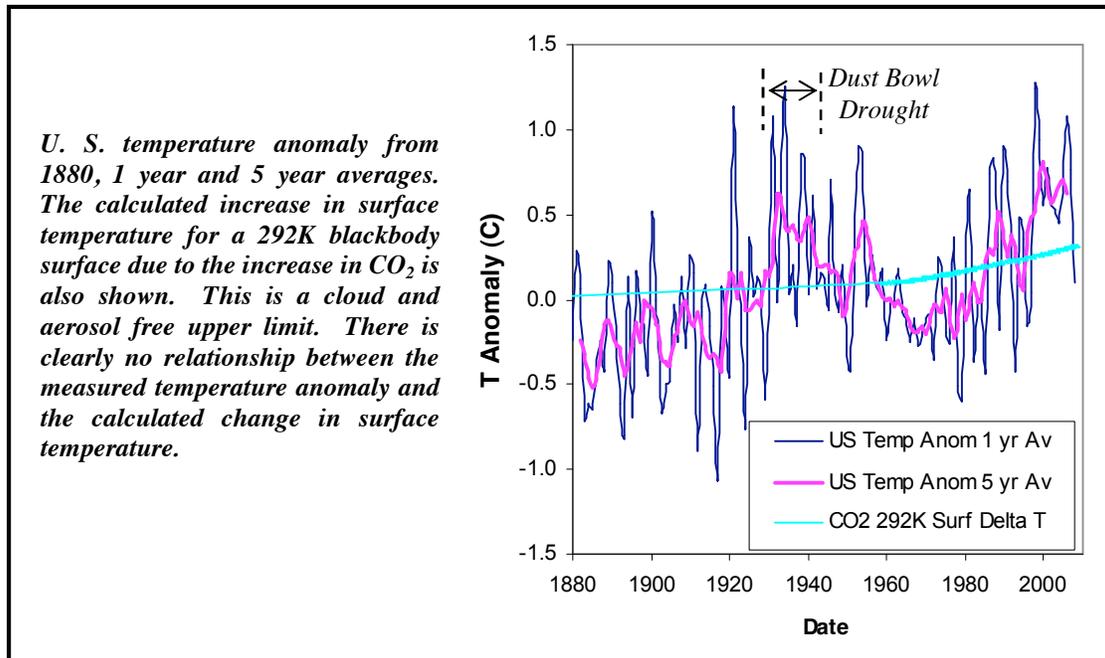
Figure 10: U. S. Temperature anomaly and calculated increase in surface temperature due to increases in atmospheric anthropogenic CO_2 concentration

Radiative Forcing

Most of the large scale climate models used to predict global warming ignore the physics of energy transfer at the Earth's surface and use an approach known as radiative forcing.[10, 23-26] This assumes that long term averages of dynamic, non-equilibrium climate variables such as radiative flux and surface temperatures can be analyzed using perturbation theory as though they were in radiative equilibrium. Although the mathematical derivation is correct and may even appear elegant, the underlying physical assumptions are invalid before the first equation is written down. The troposphere is an open thermodynamic system so heat and flux are not conserved. The temperatures in the upper troposphere are near 220 K. The assumption that small changes in LWIR flux in the upper troposphere or stratosphere can influence surface temperatures of 288 K is a flagrant violation of the Second Law of Thermodynamics. Molecular linewidths also vary with altitude because of pressure broadening, so the upward and downward LWIR fluxes are not equivalent. At the Earth's surface, radiative flux is not conserved, especially over the oceans. The calculated 'equilibrium surface temperature' is not even a physically measurable climate variable. Radiative forcing can be compared to telling the time using a broken clock.

However, in the mid 1980's, a slight increase in the 'average' meteorological surface air temperature was found.[8] This was immediately linked by empirical speculation to the increase in anthropogenic CO_2 concentration. It was decreed that a 1 $W.m^{-2}$ increase in downward LWIR flux due to an increase in atmospheric CO_2 concentration produced an increase in meteorological surface air temperature of 2/3 C.[10] Mysterious water vapor feedback effects were invoked to explain model inaccuracies. The Kirchoff exchange energy was converted into an empirical 'radiative forcing constant'. This 'calibration factor' was then applied to other greenhouse gases

such as methane and even to aerosols. The 'radiative forcing constants' in the IPCC models are devoid of physical meaning. This approach is empirical pseudoscience that belongs to the realm of climate astrology.[27] The results derived from climate simulations that use the radiative forcing approach may be of limited academic interest in assessing model performance. However, such results are computational science fiction that have no relationship to the reality of the Earth's climate. Radiative forcing by CO_2 is, by definition a self-fulfilling prophesy, since the outcome is pre-ordained with a total disregard of the basic laws of physics. An increase in CO_2 concentration must increase surface temperature. No other outcome is allowed and other possible climate effects are by definition excluded.

Based on the arguments presented here, a null hypothesis for CO_2 is proposed:

It is impossible to show that changes in CO_2 concentration have caused any climate change to the Earth's climate, at least since the current composition of the atmosphere was set by ocean photosynthesis about one billion years ago.

References

1. http://scrippsco2.ucsd.edu/data/in_situ_co2/monthly_mlo.csv. [Keeling curve data, Accessed 1/20/2009].

2. K. L. Harvey, "The solar activity cycle and sun-as-a-star variability in the visible and IR", Proc. 2nd Annual Lowell Observatory Fall Workshop, Oct 5-7, 1997, Ed. J. C. Hall, "*Solar analogs: Characteristics and Optimum Candidates*".

3. ftp://ftp.ngdc.noaa.gov/STP/SOLAR_DATA/SUNSPOT_NUMBERS/YEARLY, [Annual Sunspot Index, Accessed 3/26/2009].

4. S. Levitus, J. Antonov & T. Bower, Geophysical Research Letters **32** L02604 1-4 (2005), "Warming of the world ocean 1955-2003".

5. M. S. Lozier, S. Leadbetter, R. G. Williams, V. Roussenov, M. S. C. Reed & N. J. Moore, Science **319** 800-802 (2008), "The spatial pattern and mechanisms of heat content change in the N. Atlantic".

6. http://nsidc.org/data/smmr_ssmi_ancillary/area_extent.html#gsfc. [Ice extent data, Accessed 3/26/09].

7. R. Lindsay, W.; J. Zhang, A. Schweiger, M. Steele & H. Stern, Journal of Climate **22**(1) 165-176 (2009), "Arctic sea ice retreat in 2007 follows thinning trend".

8. P. D. Jones, M. New, D. E. Parker, S. Martin & I. G. Rigor, Rev. Geophysics **37**(2) 173-199 (1999), "Surface air temperature and its changes over the past 150 years".

9. L. S. Rothman et al, (30 authors), J. Quant Spectrosc. Rad. Trans. **96** 139-205 (2005), "The HITRAN 2004 molecular spectroscopic database".

10. J. Hansen et al, (45 authors), J. Geophys Research **110** D18104 pp1-45 (2005), "Efficacy of climate forcings".

11. http://sohowww.nascom.nasa.gov/data/data.html. [VIRGO: Near Real Time Data, Accessed 01/15/2009].

12. F. Varadi, B. Runnegar & M. Ghil, Astrophys. J. **562** 620-630 (2003), "Successive refinements in long term integrations of planetary orbits".

13. K. Lambeck, Comptes Rendus Geoscience **336** 667-689 (2004), "Sea level change through the last glacial cycle: geophysical, glaciological and paleogeographic consequences".

14. C. Barbante et al, EPICA community members, (84 Authors), Nature **444** 195-198 (2006), "One to one coupling of glacial climate variability in Greenland and Antarctica".

15. L. Augustin et al, EPICA community members, (56 Authors), Nature **429** 623-627 (2004), "Eight glacial cycles from an Antarctic ice core".

16. A. B. Robinson, N. E. Robinson & W. Soon, J. Amer. Physicians and Surgeons **12** 79-90 (2007), "Environmental effects of increased atmospheric CO_2".

17. http://floats.pmel.noaa.gov/index.html, *Argo Profiling CTD Floats*, NOAA Pacific Marine Environmental Laboratory. [Argo float data, Accessed 3/15/09].

18. G. M. Hale & M. R. Querry, Applied Optics **12** 555-563 (1973), "Optical constants of water in the 200 nm to 200 μm region".

19. L. Yu, J. Climate **20**(21) 5376-5390 (2007), "Global variations in oceanic evaporation (1958-2005): The role of the changing wind speed".

20. L. Yu, X. Jin & R. A. Weller, OAFlux Project Technical Report (OA-2008-01) Jan 2008, "*Multidecade Global Flux Datasets from the Objectively Analyzed Air-sea Fluxes (OAFlux) Project: Latent and Sensible Heat Fluxes, Ocean Evaporation, and Related Surface Meteorological Variables*".

21. R. G. Quayle, D. R. Easterlin, T. R. Karl & P. Y. Hughes, Bull Amer Met Soc **72**(11) 1718-1723 (1991), "Effects of recent thermometer changes in the cooperative station network".

22. http://data.giss.nasa.gov/gistemp/graphs/Fig.D.txt. [Contiguous 48 U.S. Surface Air Temperature Anomaly. Accessed 1/19/09].

23. S. Manabe & R. T. Wetherald, J. Atmos. Sci. **24** 241-249 (1967), "Thermal equilibrium of the atmosphere with a given distribution of relative humidity".

24. R. M. Knutti,. R. Allen, M. R. P. Friedlingstein, J. M. Gregory, G. C. Hegerl, G. A. Meehl, M. Meinshausen, J. M. Murphy, G. K. Plattner, S. C. B. Raper, T. F., Stocker, P. A. Stott, H. Teng & T. M. L. Wigley, Journal of Climate **21**(11) 2651-2663 (2008), "A Review of Uncertainties in Global Temperature Projections over the Twenty-First Century".

25. S. Solomon, G-K. Plattner, R. Knutti & P. Freidlingstein, Proc Natl Acad Sci USA **106** 1704-1709 (2009), "Irreversible climate change due to carbon dioxide emissions".

26. J. Hansen, L. Nazarenko, R. Ruedy, M. Sato, J. Willis, A. D. Genio, D. Koch, A. Lacis, K. Lo. S. Menon, T. Novakov, J Perlwitz, G. Russell, G. A. Schmidt & N. Tausnev., Science **308** 1431-1435 (2005), "Earth's energy imbalance: confirmation and implications".

27. R. B. Alley et al, (51 authors), IPCC, Summary for Policymakers, Climate Change 2007: The Physical Science Basis. Contribution of Working Group I to the Fourth Assessment Report of the Intergovernmental Panel on Climate Change [Solomon, S., D. Qin, M. Manning, Z. Chen, M. Marquis, K.B. Averyt, M.Tignor and H.L. Miller (eds.)]. Cambridge University Press, Cambridge, United Kingdom and New York, NY, USA.